Soft Matter

PAPER

Cite this: *Soft Matter*, 2015, **11**, 389

Structural heterogeneity of milk casein micelles: a SANS contrast variation study†

Antoine Bouchoux,‡*[ab] Jorge Ventureira,[ab] Geneviève Gésan-Guiziou,[ab] Fabienne Garnier-Lambrouin,[ab] Peng Qu,[ab] Coralie Pasquier,[ab] Stéphane Pézennec,[ab] Ralf Schweins[c] and Bernard Cabane[d]

We examine the internal structure of milk casein micelles using the contrast variation method in Small-Angle Neutron Scattering (SANS). Experiments were performed with casein dispersions of different origins (*i.e.*, milk powder or fresh milk) and extended to very low q-values ($\sim 9 \times 10^{-4}$ Å^{-1}), thus making it possible to precisely determine the apparent gyration radius R_g at each contrast. From the variation of $I(q \rightarrow 0)$ with contrast, we determine the distribution of composition of all the particles in the dispersions. As expected, most of these particles are micelles, made of casein and calcium phosphate, with a narrow distribution in compositions. These micelles always coexist with a very small fraction of fat droplets, with sizes in the range of 20–400 nm. For the dispersions prepared from fresh milk, which were purified under particularly stringent conditions, the number ratio of fat droplets to casein micelles is as low as 1 to 10^6. In that case, we are able to subtract from the total intensity the contribution of the fat droplets and in this way obtain the contribution of the micelles only. We then analyze the variation of this contribution with contrast using the approach pioneered by H. B. Stuhrmann. We model the casein micelle as a core–shell spherical object, in which the local scattering length density is determined by the ratio of calcium phosphate nanoclusters to proteins. We find that models in which the shell has a lower concentration of calcium phosphate than the core give a better agreement than models in which the shell has a higher density than the core.

Received 1st August 2014
Accepted 29th September 2014

DOI: 10.1039/c4sm01705f

www.rsc.org/softmatter

Introduction

The milk casein micelle is one of those natural and ordinary colloids that have always been part of our everyday life. But despite this apparent familiarity, the casein micelle still remains a mysterious and fascinating object for (bio)physicists. The recurrent question of its internal structure, which has been the subject of a myriad of papers and reviews in the last 50 years,[1–9] is surely the best illustration of this. In the present paper, we aim at giving novel information about that very question. The approach followed is essentially based on the 1974 influential work of H. B. Stuhrmann[10] and involves precise experiments of Small-Angle Neutron Scattering (SANS) at varying contrasts.

Casein micelles are globular particles of sizes mostly comprised between 50–200 nm.[11,12] They result from the association of four types of casein (denoted as α_{s1}-, α_{s2}-, β-, and κ-) together with 7–8% in dry mass of phosphate and calcium ions;[13] the latter being in the form of amorphous CaP nanoclusters.[2,6,14] Besides proteins and minerals, the casein micelle also contains a large amount of water (~3–4 g per g of caseins),[15] a constituent that presumably plays a central role in micellar stability.[1] How these constituents are arranged within the micelle is a crucial question for at least two reasons: (i) it is obviously important to gain new fundamental knowledge about this biological object, thus contributing to some other fascinating questions such as milk secretory process and micelle assembly in lactating cells.[16,17] (ii) The performance of many dairy processes, as well as the quality of many dairy products, is intimately linked to the structural properties of the casein micelle.[18–21] Also it is decisive to identify and understand these properties if one wants to develop new applications, such as the promising use of casein micelles for drug delivery.[22]

Various methods of investigation have been used for studying the structure of the casein micelle in the past decades, among which three were clearly privileged: the biological route,

[a]*INRA, UMR1253 Science et Technologie du Lait et de l'Œuf, F-35042 Rennes, France. E-mail: Antoine.Bouchoux@insa-toulouse.fr*

[b]*Agrocampus Ouest, UMR1253 Science et Technologie du Lait et de l'Œuf, F-35042 Rennes, France*

[c]*Institut Laue-Langevin, DS/LSS group, F-38042 Grenoble Cedex 9, France*

[d]*Laboratoire CBI, CNRS UMR8231, ESPCI, 10 rue Vauquelin, F-75231 Paris Cedex 05, France*

† Electronic supplementary information (ESI) available. See DOI: 10.1039/c4sm01705f

‡ Present address: Laboratoire d'Ingénierie des Systèmes Biologiques et des Procédés/LISBP, UMR5504/792 INRA-CNRS-INSA, 135 avenue de Rangueil, F-31077 Toulouse Cedex 04, France.

i.e., the study of how the micelle assembles in the lactating cell through biochemistry techniques,[16,17,23] the direct imaging of the micelle through microscopy techniques,[7,8,12,24] and the visualization in reciprocal space and subsequent modeling of the edifice through Small-Angle Neutron or X-ray Scattering (SANS, SAXS) experiments.[2,3,6,24] Much progress has been achieved in recent years, so that some structural features are now well-identified, such as the presence of a κ-casein brush layer at the micellar surface, or the size and average distance between CaP nanoclusters, for instance. There is, however, still no consensus on the exact repartition of casein, water, and CaP nanoclusters in the micelle, with a diversity of pictures ranging from the fully homogeneous casein network with randomly or radially distributed CaP nanoclusters,[3,6,13,24–26] to the heterogeneous sponge-like micelle made from dense casein/CaP regions separated by water cavities.[1,2,7,8]

In order to contribute to the discussion in a constructive way, it is necessary to provide new and precise experimental information about possible structural heterogeneities in the micelle. To this aim, SANS contrast-variation, which is based on the distinct interaction of neutrons with hydrogen and deuterium atoms,[27] is a method of choice. By substituting H for D to various degrees, it is indeed possible to change the Scattering-Length Density (SLD) of the solvent relative to that of the particle investigated and its constituents. The way the SANS signal changes with the degree of H–D substitution (*i.e.*, contrast) provides unique information about the structure and composition of the particle. In the region of low scattering angles, such changes can be followed through the variation of the Guinier parameters R_g and I_0, which are the radius of gyration of the particle and the corresponding zero-angle scattering intensity, respectively. As first demonstrated by H. B. Stuhrmann in the late 70s,[10,27] the variation in R_g with contrast gives access to the radial SLD distribution within the particles, while the variation in I_0 gives an evaluation of the average composition of the particles (for a detailed illustration of this method, we refer the reader to the didactic work of Stuhrmann on ferritin,[10] a protein that is able to store iron and therefore naturally presents inter- and intra-individual variations in SLD). In the case of the casein micelle, a Stuhrmann analysis of the radius of gyration seems particularly appropriate for examining how the CaP nanoclusters are distributed within the micellar edifice. If this distribution is fully random and uniform, the measured radius of gyration will be the same at all contrasts. If this distribution is of the core–shell type, then the curvature of the intensity at low q, usually described as an apparent squared radius of gyration, R_g^2, will depend on contrast. In this case, the curvature of the intensity may even take negative values near the contrast match point of the micelle, which requires the apparent radius of gyration R_g to take imaginary values.[10]

In the past 30 years, a few pioneers have studied casein micelle dispersions through SANS contrast variation experiments.[3,13,28–31] However, these experiments did not reach the very low q values that are necessary to perform an accurate Stuhrmann analysis, particularly at lower contrast values. In this paper, we precisely address this issue using SANS data obtained with casein micelles at 12–15 contrast points, and in an exceptionally low q-range of $\sim 1 \times 10^{-3}$ to 1×10^{-2} Å^{-1}. Experiments were performed with both native casein micelles that were carefully extracted from fresh milk, and casein micelles obtained from a milk powder, the latter being often used as a model even though the micelles are then potentially damaged through drying and subsequent rehydration. In each case, the variation of I_0 and of the apparent radius of gyration R_g with contrast is reported. We then provide a detailed analysis of these results, with the intention to answer the following questions:

(1) How do R_g and I_0 change with contrast? Does this variation depend on the origin of the casein micelle (fresh milk *versus* powder)? Is the variation in I_0 consistent with what we know about the average composition of a casein micelle?

(2) Does the variation in R_g really provide new information about the CaP distribution within the casein micelle? Are we capable of finding a structural model that quantitatively predicts the observed variation in R_g?

(3) With this work, are we finally able to validate or invalidate some of the models that are currently in use for the casein micelle?

Experimental

Casein micelles

Casein micelles were taken from two different sources: extra fresh milk (FM) and native phosphocaseinate (NPC) powder. By using fresh milk, our intention was to obtain casein micelles as close as possible to their native state, and special efforts were made in this direction (no cooling or drying for instance, see the next subsection for details). On the other hand, samples were also prepared from NPC powder because NPC is routinely used as a model for native milk casein micelles.[25,26,32,33] Also we found it interesting to confront this model with *intact* casein micelles extracted from fresh milk.

The fresh milk was provided by a farm in Montgermont, France, where it was collected in the morning from three different cows and subsequently mixed. The milk was then transported to our laboratory at ambient temperature. There it was carefully skimmed at 40 °C using a milk centrifuge (Elecrem 30). Thimerosal and sodium azide, both purchased from Sigma-Aldrich, were finally added to it as preservatives at concentrations 0.02 g L^{-1} and 0.5 g L^{-1}, respectively.

The NPC powder was prepared in our laboratory according to a protocol developed by Pierre *et al.*[34] and Schuck *et al.*[35] and briefly described in a previous study.[36] In such a powder, the caseins and their associated minerals represent >90% of the total solid content. For preparing casein micelle dispersions, the powder was dispersed in a solvent made from the ultrafiltration (5 kDa cutoff) of skim milk, with subsequent stirring at 35 °C overnight. Thimerosal and sodium azide were added to the final NPC dispersion at the same concentrations as above.

Sample preparation

Table 1 lists the samples prepared for this study. Each line corresponds to a different sample set, with its average casein

concentration, the radius of gyration as measured through SANS at 0% D_2O ($x_{D_2O} = 0$), and the different contrasts (D_2O contents) that were investigated. Two SANS experimental sessions were performed: one in May–June 2011 (sample sets "_s1") and the other in September 2012 (sample sets "_s2").

To each sample set in Table 1 corresponds a stock solution of casein micelles. This stock solution was prepared either from a fresh skim milk or from a NPC dispersion:

• In the case of fresh milk (FM), the casein micelles were first separated from the serum proteins that also compose milk (mainly β-lactoglobulin and α-lactalbumin). This was done through two successive centrifugations performed at 45 000*g* for 1 h each (Sorvall Discovery 90 SE, Hitachi, $T = 20$ °C; see the ESI, part A,† for a brief discussion about the chosen conditions of centrifugation), with the pellet being each time re-dispersed in a 5 kDa filtrate of skim milk. Importantly, and because fat has lower density than water, these two centrifugations also have the effect of further purifying the casein dispersion with respect to fat globules that possibly remain after skimming. The resulting solution was then centrifuged again at 30 000*g* to remove any possible casein aggregates in the pellet (20 °C, 30 min to 1 h). The solution was finally adjusted to a casein concentration of ~45–60 g L^{-1} through the addition of a small volume of skim milk ultrafiltrate.

• In the case of NPC, and because the NPC powder already lacks the milk serum proteins, the dispersion was only gently centrifuged at 15 000*g* and 20 °C for 15–30 min in order to remove any possible casein aggregates. The final NPC stock solution was adjusted to a casein concentration of ~45–50 g L^{-1}.

• In all cases, the precise casein concentration of the stock solution was determined accurately through drying at 105 °C.

In parallel, stock solutions of so-called *simulated* milk ultrafiltrate (SMUF) were prepared according to a protocol given by Jenness *et al.*[37] SMUF solutions are designed to have the same pH (or pD) and ionic composition as milk, *i.e.*, pH/pD 6.6, ~20 mM Na^+, ~40 mM K^+, ~10 mM Ca^{2+}, ~30 mM Cl^-, ~10 mM phosphate, and ~10 mM citrate. The SMUF was prepared either with ultra-pure H_2O or 99.8% pure D_2O (Sigma-Aldrich) as the aqueous phase. Both SMUF_H_2O and SMUF_D_2O were then kept at 4 °C to inhibit calcium phosphate precipitation or crystal growth.[38] The SMUFs were put back at room temperature a few hours before preparation of the casein samples.

The samples for SANS analysis were prepared at D_2O contents ranging from 0 to 80% by diluting 1 : 5 the stock solutions of casein micelles with given volumes of SMUF_H_2O and SMUF_D_2O. The SMUFs were filtered through 0.1 μm syringe filters (Pall Corporation) just before use in order to remove any mineral precipitates or crystals that would pollute the SANS signal. The final D_2O content of the samples was determined by weighing each SMUF addition during preparation.

Specific samples were also prepared to examine if a residual SANS signal exists after casein removal. This was done by precipitating the caseins at pH 4.6 with HCl in a given volume of the NPC_s2 stock solution. The resulting solution was then centrifuged at 70 000*g* for 30 min to fully remove the precipitated caseins. The samples were finally prepared by diluting 1 : 5 the supernatant in SMUF_H_2O and SMUF_D_2O solutions that were also acidified to pH/pD 4.6 beforehand.

All samples were prepared at casein concentrations around $C \approx 10$ g L^{-1}, a concentration at which SANS intensities can be recorded within reasonable acquisition times, and where the Guinier parameters R_g and I_0/C are still not affected by interparticle scattering contributions (results not shown). Also all samples were prepared between 10–15 hours before SANS analysis, a time that is sufficiently long to allow full H–D exchange (as verified by following the scattered intensity just after sample preparation, data not shown), and during which contamination or destabilization phenomena still do not occur. It is important to note here that deuteration has no significant effect on the structure of the casein micelle. This was checked through additional SAXS experiments that we performed on casein micelles at various D_2O contents and that we report in ESI part B.†

Finally, the samples were always prepared and kept at room temperature (20–25 °C) as we know that the casein micelle is quite sensitive to changes in temperature, especially towards low temperatures.[1]

Small-Angle Neutron Scattering (SANS)

The SANS experiments were performed on the D11 instrument, Institut Laue-Langevin (ILL), Grenoble, France. The samples were placed in 1 mm path length quartz cells (Helma Analytics),

Table 1 Summary of the samples investigated in this study

Sample type	Given name[a]/Stock solution	Casein conc. (g L^{-1})	R_g (Å) at $x_{D_2O} = 0$	x_{D_2O} (%)
Casein micelles from fresh milk	FM_s1	~12.5	690 ± 10	0, 15, 25, 30, 35, 37, 38, 40, 42, 45, 47, 51, 56, 66, 81
	FM_s2	~9.5	785 ± 10	0, 12, 25, 35, 40, 42, 44, 46, 50, 60, 70, 81
Casein micelles from casein powder	NPC_s1	~10	685 ± 12	0, 28, 34, 35, 38, 40, 43, 46, 48, 50, 53, 55, 80
	NPC_s2	~9.5	780 ± 12	0, 12, 25, 35, 40, 42, 45, 47, 51, 61, 71, 81
Residual signal after casein precipitation	NPC_s2_Residual	0[b]	—	0, 20, 30, 40, 50, 60, 70, 80

[a] Samples "_s1" were analyzed through experiments performed in May–June 2011 on D11, ILL. Samples "_s2" were analyzed in September 2012, still on D11. [b] The samples do not contain casein anymore but are prepared using the same dilution procedure than for the other series, *i.e.*, 1 : 5 of the stock solution in the SMUF.

positioned in a sample rack thermostated at 25 °C. All the data presented in this paper are from intensities collected at neutron wavelengths λ = 12–13 Å and at sample-to-detector distances 34–39 m. These intensities were radially averaged and arranged as a function of scattering vector q, leading to $I(q)$ spectra in the range of $q = \sim 9 \times 10^{-4}$ to 1×10^{-2} Å^{-1}. In all cases, corrections were made for instrumental background, empty cell, and transmission. Sample background was determined from the (flat) intensity signal of pure SMUF solutions at various D_2O contents, hence enabling background subtraction at any desired D_2O concentration. Normalization to absolute intensities was achieved by using H_2O as a second calibration standard cross-calibrated against H/D polymer blends.

The SASfit software (vers. 0.93.5) was used for data modeling and SLD calculations,[39] and the PRIMUS software (ATSAS 2.5.1) was used for Guinier analysis.[40] In order to have robust and reliable values of R_g and I_0, all datasets were analyzed following the exact same procedure, focusing in each case on the signal acquired at $q^2 < 5 \times 10^{-6}$ Å^{-2} (Fig. 1). The high-q limit of this range was chosen low enough to ensure that the higher order terms of the Guinier approximation for dense particles are still quite small, but still high enough to incorporate a sufficient number of points (11–14 points) in the fits. The reported values of R_g and I_0 and their associated standard deviations are average values obtained from three Guinier fits: one fit performed with the totality of the points in the above mentioned q-range and two other fits performed by discarding either the first two or the last two experimental points in the chosen q-range.

Results

Casein micelles from fresh milk

Fig. 1 shows the raw SANS intensities for casein micelles extracted from fresh milk (FM_s1, Table 1) and measured at 15 contrast points. The intensity profiles measured with the other set of fresh milk samples (FM_s2) are qualitatively similar to those in the FM_s1 set and are shown in ESI part C.† Also for simplicity, only the results obtained at low q-values are reported. They are given in the form of Guinier plots (semi-log plot of I *vs.* q^2), where Guinier's approximation (eqn 1) gives straight lines of slope $-{R_g}^2/3$:

$$I(q) = I_0 \exp\left(-\frac{q^2 {R_g}^2}{3}\right) \quad (1)$$

The Guinier fits are entirely satisfactory for all contrasts. This is the first important point here as it indicates that the I_0 and R_g values that are discussed in this paper are relevant and reliable. The second interesting observation, which is analyzed further in the following, is that the slope of the signal takes different values in the region of low contrast (Fig. 1(B)).

The I_0 values obtained from the Guinier analyses are given in Fig. 2 for both experimental series FM_s1 and FM_s2. As it is commonly done in contrast variation studies, the square root of the intensity is reported as a function of D_2O content. Also the intensity is normalized by the concentration of casein in the sample, as the quantity of casein was not exactly the same in each case. For comparison, the I_0 values that were recently reported by de Kruif *et al.* for similar dispersions of casein micelles are given in Fig. 2(A).[3]

Our data, as those of de Kruif, indicate that the scattered intensity never vanishes at a given content of D_2O but rather passes through a minimum value. The D_2O content at which this minimum value is reached can be estimated from a simple linear regression, as depicted in Fig. 2. The obtained points of minimum contrast are $x_{D_2O} = 0.432$ and 0.440 for the two series (the data of de Kruif do not allow to make this regression in an

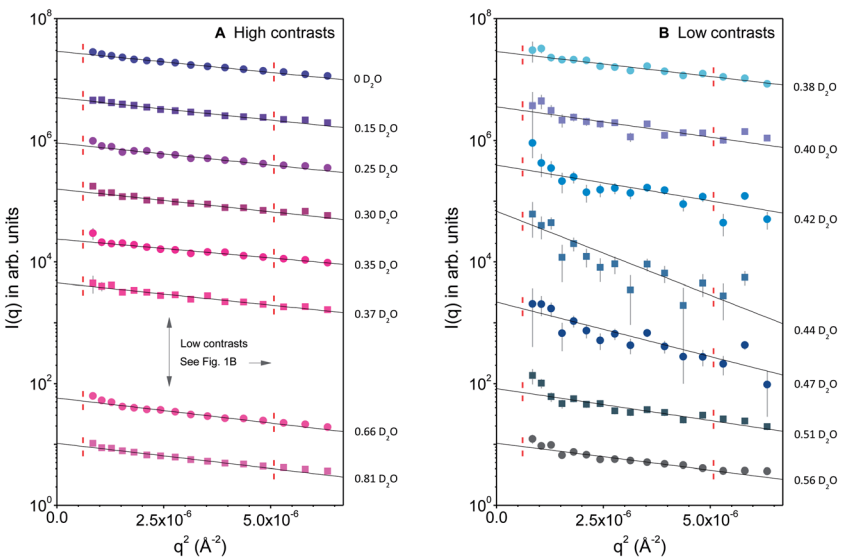

Fig. 1 The Guinier plots from the SANS intensities of casein micelles of fresh milk at various D_2O/H_2O compositions (experimental series FM_s1, Table 1): (A) results obtained at high contrast, *i.e.*, at the lowest and highest D_2O contents and (B) low contrast, *i.e.*, where x_{D_2O} is close to the contrast match point of an average casein micelle (estimated at $x_{D_2O} \approx 0.446$, see ESI part D†). The vertical dashed lines indicate the q-range used for the Guinier analyses. The intensities were shifted along the y-axis for clarity.

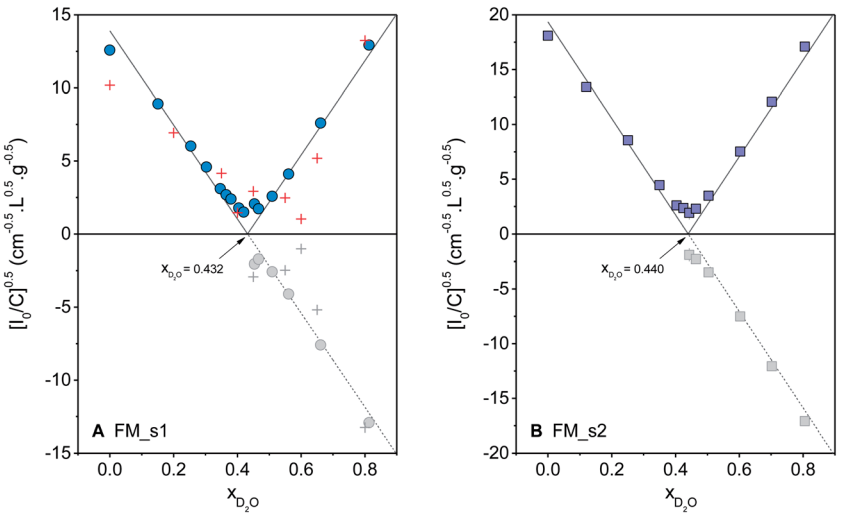

Fig. 2 Variation of the square-root of the zero-angle intensity as a function of D_2O content for dispersions of casein micelles from fresh milk: (A) FM_s1 and (B) FM_s2. The intensities are normalized by the concentration of casein in the sample. For comparison, the values reported by de Kruif *et al.* for a similar system are given in (A) as crosses.[3] The D_2O volume fraction at minimum contrast is determined from a linear regression of the data, taking as negative the $\sqrt{I_0/C}$ values obtained at negative contrast (*i.e.*, when the solvent SLD is supposedly lower than the particles SLD, shaded symbols).

acceptable manner). These values are clearly in accordance with the match points estimated experimentally by other groups (yet with much less contrast points, $x_{D_2O} = 0.38$–0.41[28,30]). They are also very close to the match point estimated from the average composition of the micellar part of milk ($x_{D_2O} = 0.446$, see ESI part D†).

Fig. 3 shows the variation of R_g with contrast for the same dispersions of casein micelles from fresh milk. At high contrast, R_g is stable around 700 Å (FM_s1) and 800 Å (FM_s2). These values are consistent with the dimension usually reported for the casein micelle, as measured through DLS for instance.[11] At low contrast, and as it was effectively suggested in Fig. 1(B), R_g is no longer constant and increases significantly (almost twofold) when approaching the point of minimum contrast. This increase is restricted to a short range of D_2O content, *i.e.*, $x_{D_2O} = 0.4$–0.5.

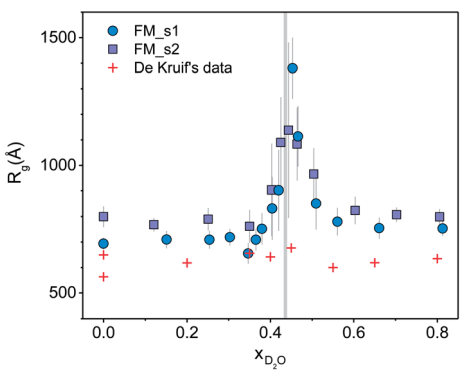

Fig. 3 Variation of R_g as a function of D_2O content for dispersions of casein micelles from fresh milk. The R_g values reported by de Kruif *et al.* are given for comparison.[3] The shaded area gives the x_{D_2O} region where contrast is at its minimum, as obtained from Fig. 2(A and B).

The R_g values of de Kruif *et al.* are also given in Fig. 3.[3] In the range $x_{D_2O} = 0.4$–0.5, the two points obtained by these authors indicate that R_g does not vary substantially. The standard deviation associated with these points is however not specified. In addition, the R_g value reported by de Kruif at $x_{D_2O} = 0.45$ corresponds to a zero angle intensity that is abnormally high (Fig. 2(A)). It is then plausible that this specific value is not fully reliable.

Casein micelles from casein powder

The SANS spectra obtained with dispersions of casein micelles prepared from a casein powder are given in ESI part C.† Fig. 4 provides the results of the Guinier analysis of these spectra.

Clearly, I_0 and R_g vary in a way that is very close to the one observed with samples prepared from fresh milk: I_0 has a minimum value that is not zero and R_g varies noticeably in the region of low contrast. However, some interesting and systematic differences exist between the two types of samples. Concerning the variation of I_0 (Fig. 4(A)), the first difference is that the point of minimum contrast is positioned a lower D_2O content when the origin of the samples is a powder ($x_{D_2O} \approx 0.39$–0.41). Furthermore, the overall level of intensity at minimum contrast is noticeably higher in this case, with $\sqrt{I_0/C} = 3.5 - 5.2$ cm$^{-0.5}$ L$^{0.5}$ g$^{-0.5}$ against 1.5–1.9 cm$^{-0.5}$ L$^{0.5}$ g$^{-0.5}$ for casein dispersions from fresh milk. Concerning the variation of R_g with contrast (Fig. 4(B)), the differences are threefold. First, the increase in R_g is less marked and does not exceed $\times 1.5$ for the NPC series. Second, the range of D_2O content where R_g varies is much wider in this case. Third, and in contrast to the fresh milk series, there is for NPC a clear mismatch between the contrast at which R_g is maximum and the point of minimum contrast as determined through a linear regression of I_0.

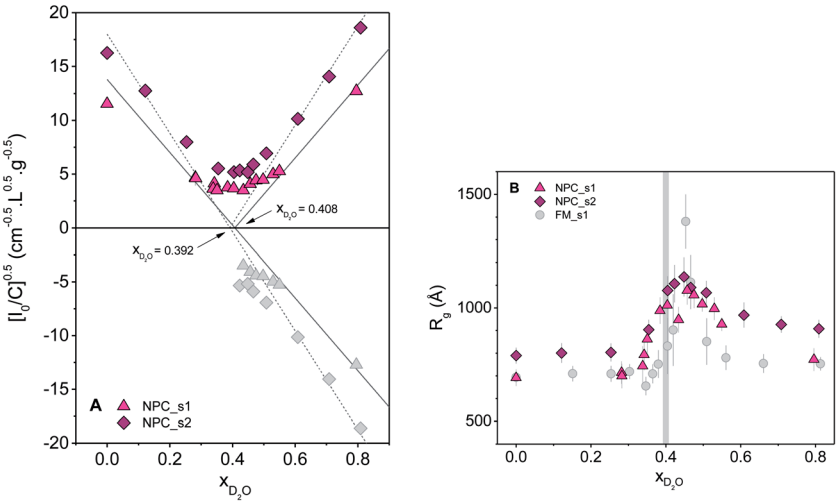

Fig. 4 Variations of $\sqrt{I_0/C}$ and R_g as a function of x_{D_2O} for casein micelles from casein powder (NPC). The shaded area in (B) is the region where contrast is minimum, as obtained from (A). For comparison, the results obtained with casein micelles from fresh milk (FM_s1) are reported in (B).

Residual signal after precipitation of the caseins

For both types of casein micelle samples, *i.e.*, fresh milk or powder, our results indicate that I_0 never vanishes but rather passes through a minimum value that is not zero. This can have two origins: (i) the composition of the casein micelles varies from one micelle to another and (ii) the dispersions not only contain casein micelles, but also other objects of distinct SLD. In order to examine hypothesis (ii), SANS experiments were performed with samples in which the casein micelles were precipitated at low pH and then eliminated through centrifugation (see the Experimental section). The stock solution of the experimental series NPC_s2 was used and samples with D_2O contents ranging from 0 to 0.8 were prepared (Table 1).

At $x_{D_2O} < 0.4$, no SANS signal was detectable. As $x_{D_2O} \geq 0.4$, a SANS signal was detected, indicating that objects other than casein micelles are indeed present in the dispersion. This signal can be successfully analyzed according to Guinier's approximation (ESI part C†), so that we can estimate the zero angle intensity and its variation with D_2O content (Fig. 5(A)).

The variation of I_0 with contrast suggests that the residual objects are matched near $x_{D_2O} \approx 0.10$, which is in the range of match points usually reported for lipids or phospholipids.[27,42] We thus suppose that these objects are residual small fat globules or droplets that were not eliminated from the dispersions by centrifugation. Part of these objects could also be process-induced phospholipid vesicles like those described by Waninge *et al.*[43] Such vesicles result from the partial breakdown of the milk fat globule membrane during the process of separating the casein micelles from milk. Both types of structure can be used in a form factor model for describing the experimental results (Fig. 5(B)). Note that the intensities measured before and after casein removal are significantly different at the theoretical match point of the casein micelle ($x_{D_2O} \approx 0.446$), while one would expect about the same value at that peculiar point. This difference is in fact not surprising since the protocol followed for removing the casein micelles from the samples has not been optimized and most probably leads to some loss of residual fat globules and/or phospholipid vesicles.

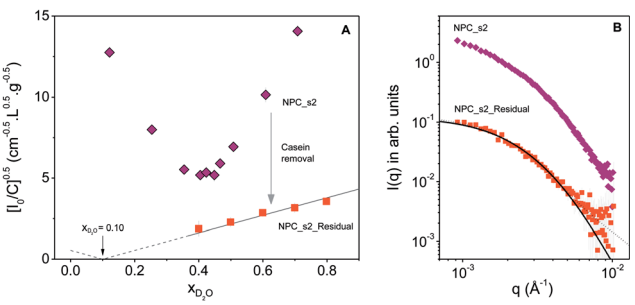

Fig. 5 Residual signal after precipitation of the casein micelles. (A) Variation of $\sqrt{I_0/C}$ as a function of x_{D_2O} for NPC_s2 before and after removal of the caseins. (B) The SANS intensities at $x_{D_2O} = 0.8$ before and after removal of the caseins. The full line is the form factor for spheres with sizes following a log-normal distribution centered at a number-average value of $\bar{R}_{spheres} = 229$ Å and a polydispersity index of $\sigma = 0.5$. The dotted line is the form factor for vesicles of constant shell thickness 60 Å[41] and with core sizes following a log-normal distribution with $\bar{R}_{ves,core} = 303$ Å and $\sigma = 0.5$.

Discussion

Summary of the problem

The experimental results given in the previous section constitute a precise and complete set of R_g and I_0 data for the casein micelle in SANS contrast variation. These results were obtained with casein dispersions of different origins and during two distinct experimental campaigns. In all cases, the variations of R_g and I_0 with contrast show a variety of common and distinct features, which is now necessary to understand and elucidate.

As regards to the variation of I_0 with contrast, the central information is that I_0 always goes through a minimum value that is not zero, whatever the origin of the casein dispersions.

This directly indicates that the objects that coexist in the dispersions do not have identical compositions. In ESI part E,† we demonstrate that this composition heterogeneity cannot be explained by the natural distribution in composition of the casein micelles in milk, which is in fact too small to be detectable in SANS experiments. On the other hand, we have clear experimental evidence that objects other than casein micelles are present in the dispersions (most probably residual fat globules and/or phospholipid vesicles). So clearly here, the main question is about the exact contribution of these non-casein objects to the SANS intensities, and whether or not their presence is sufficient for explaining the measured variation of I_0 with contrast.

As regards to the variation of the R_g with contrast, our results indicate that R_g increases in the region of low contrast, again whatever the origin of the samples. Following Stuhrmann's work, and in the ideal case of a dispersion of one single object, such a variation of R_g indicates that there exists a variation of mass distribution within the particle.[10] In the present case, and as just pointed out, the casein micelles are not alone in the dispersion but are accompanied by non-casein particles that have a distinct SLD. *A priori*, it is difficult to know what can be the effect of this coexistence on the variation of R_g. So here again, the first challenge is to determine the exact contribution of the non-casein objects to the observed variation of R_g with contrast. Once this contribution is known, the purpose is to understand what the R_g variation actually tells us about the internal structure of the casein micelle.

In the following discussion, we address these different issues based on the simultaneous and direct modeling of the variation of I_0 and R_g with contrast. In all the calculations, we consider that the H–D exchange has no impact on the size and internal structure of the casein micelles, as indicated by SAXS measurements (ESI part B†). A detailed description of the models is provided in ESI part F.†

The simple case: all the casein micelles have the same homogeneous composition

In this first case, we compare the experimental data to the simple model where there is no variation in SLD within the casein micelle. The micelles are assimilated to polydisperse spheres having a radial SLD profile that is perfectly flat. As the effect of the distribution in composition between the micelles is negligible (ESI part E†), we assume that they all have the same composition. Finally, the micelles are assumed to coexist with a certain number of lipid objects (fat droplets or phospholipids vesicles) with a contrast match point at $x_{D_2O} = 0.10$. The adjustable parameters of the model are the size characteristics of the casein micelles and lipid objects, as well as the mass ratio fat/casein in the dispersion. Both R_g and I_0 are calculated by the model and the above mentioned parameters are varied so that both experimental variations of R_g and I_0 are best described by the model. Fig. 6 shows the results of the fits for two experimental series: FM_s1 and NPC_s2. The results for all the series are given in ESI part F (Fig. S8–S11,† homogeneous model).

In all cases, the model is able to reproduce the variation of I_0 in a quite accurate manner. Also the model gives minimum values of I_0 that are always very close to the experimental ones. The presence of objects of contrast match $x_{D_2O} = 0.10$, probably made of fat, then appears to be sufficient for describing the I_0 results. The mass ratios fat/casein obtained by the fits are given in Tables S2–S5 of the ESI.† When the residual fat is assumed to be constituted of fat droplets, the estimated ratios are between 0.002–0.02% for the dispersions prepared from a fresh milk, and between 0.15–0.3% for the dispersions made from a NPC powder. In this last case, the obtained quantities are similar to the residual fat content that is usually reported for NPC powders.[44] As for the FM series, it is coherent to find smaller fat quantities as the succession of operations performed for preparing the samples is much more favorable to the effective elimination of fatty materials (through centrifugation pelleting in particular). When considering that the residual fat is made of phospholipid vesicles, the estimated fat/casein ratios are ten times larger than those estimated assuming fat droplets. Such concentrations are too high to be realistic, which suggests that the residual fat is mainly if not totally organized into fat droplets.

Still concerning I_0, we note that some small and systematic differences however exist between the model and the experiments. First, the model always overestimates the intensity at $x_{D_2O} < 0.2$ and it is thus unable to reproduce the little asymmetry of the experimental variation of I_0 with contrast. The second difference lies in the minimum I_0 values of the model, which are always slightly smaller than the experimental ones.

Fig. 6 indicates that the model is also very good in describing the experimental variation of R_g with contrast (see also Fig. S8–S11 in the ESI†). So again, the presence of residual fat droplets in the dispersion seems sufficient to explain the experimental results. At low D_2O content, the contribution of the droplets to the total scattered intensity is low, so that the neutrons do not "see" the droplets. The measured R_g is then the equivalent R_g of the population of casein micelle, which is polydisperse (polydispersity index 0.1–0.15), and centered at a hydrodynamic radius of 800–1000 Å (Tables S2–S5 in the ESI†). As x_{D_2O} increases and approaches the point of contrast match of the casein micelle, the contribution of the fat droplets to the scattered intensity becomes more important. The measured radius of gyration then gets closer to the equivalent R_g of the population of residual fat droplets, which are probably highly polydisperse in size (Fig. 5(B)), but overall slightly larger than the micelles. Quite obviously, this effect is maximum at the match point of the micelle. It then gets smaller as x_{D_2O} continues to increase and the contribution of the casein micelles to the total intensity rises again.

As opposed to I_0, there is no systematic difference between the model and the experiments in the case of the R_g. Only small deviations exist in some places. It is the case for the FM_s1 series for instance, where R_g is slightly underestimated at high D_2O content (Fig. 6(B)).

A last but interesting remark concerns the amount of fat that is associated with the rise in R_g at low contrast. The sample series FM_s1 is the one for which the concentration in fat

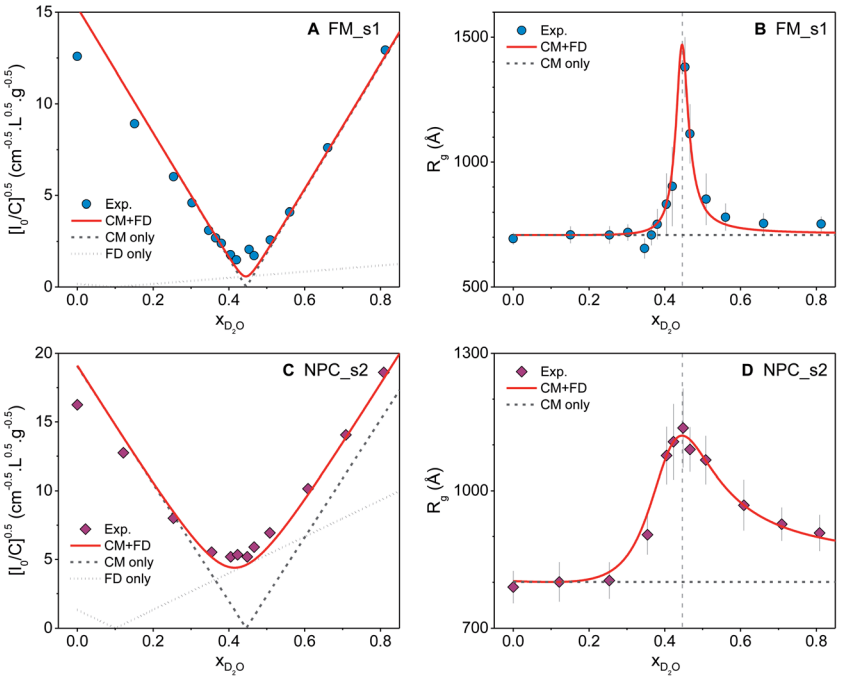

Fig. 6 Modeling the variation of $\sqrt{I_0/C}$ and R_g with contrast for dispersions of casein micelles obtained from fresh milk ((A and B), FM_s1) and casein powder ((C and D), NPC_s2). The casein micelle (CM) is supposed to have a constant radially averaged SLD distribution (homogeneous model) and to be surrounded by small fat droplets (FD). The full line is the model, while the dashed and dotted lines are the individual contributions of CM and FD, respectively. The vertical dashed line in (B and D) indicates the contrast match point of the CM ($x_{D_2O} = 0.446$).

droplets is the smallest, *i.e.*, 0.002% in total dry mass (Table S2 in the ESI†). In this case, as in the others, the effect of the presence of the droplets on the contrast variation of R_g is obvious. However, from our estimations, 0.002% in mass corresponds to a number of fat droplets that is exceptionally low, with 1 fat droplet for 10^6 casein micelles (!). Very small quantities of impurities then appear to be sufficient to produce large effects on the variation of the R_g. The problem is of course general for all systems in SANS contrast variation. In the specific case of casein micelle dispersions, its magnitude is greatly exacerbated because (1) the impurities and casein micelles have very distinct SLDs and (2) the impurities are overall larger than the micelles.

Refining the picture: heterogeneous casein micelles with a core–shell SLD distribution

So far we have assumed that the dispersions contain micelles with a homogeneous SLD (on a radially averaged basis), coexisting with a very small amount of fat droplets that also have a homogeneous SLD. The good agreement with SANS results could be taken to imply that the micelles have a flat radial SLD profile, as in models where they are made of fully homogeneous casein/CaP networks,[3,13,24,26] or in models where they are made of a sponge-like material with a homogeneous casein/CaP composition and randomly distributed aqueous cavities.[1,2,7,8] On the other hand, it is also possible that the radial distribution of SLD within the micelle is not uniform, and that such a distribution would lead to an even better description of our SANS results. In the following, we examine this alternative by considering casein micelles that have core–shell structures. We compare two types of structures, both of them inspired from the literature.

The first non-homogeneous structure (core–shell 1) takes into account the presence of a κ-casein brush at the micelle surface.[45] Since κ-caseins have little affinity towards CaP nanoclusters, this model assumes that the κ-casein brush does not contain any CaP. The micelle is then described as a core–shell object, with the same casein concentration everywhere, but with all the CaP nanoclusters located in the core. The second non-homogeneous structure is the one proposed by Shukla *et al.* in a recent SAXS study of casein micelles in the presence of tannins.[6] The authors explain their results by the preferential localization of CaP nanoclusters at the periphery of the micelle, *i.e.*, in the vicinity of the κ-casein brush. We simplify this fairly complex model as a core–shell structure (core–shell 2) where the core and shell have distinct but uniform electronic density. The shell is about 12 nm thick and has an electronic density that is ×1.2–1.5 superior to the one of the core. From our estimations, this difference in electronic density implies that the shell contains 5 to 10 times more CaP nanoclusters than the core, information that we can convert into differences in SLD between the core and the shell.

Using these two core–shell structures, we construct models similar to the one described previously and we calculate the variation with contrast of the intensity produced by the total population of casein micelles and residual fat droplets (see ESI part F† for details about the calculations). The fits of these models to the experimental values are given in Fig. S8–S11 of ESI part F.† Concerning the variation of I_0, the two core–shell

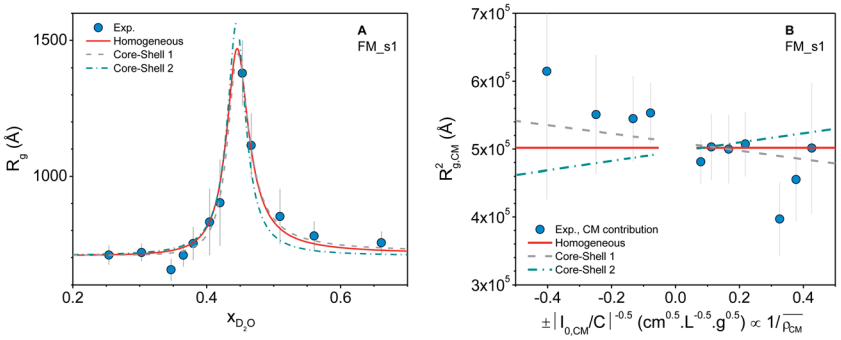

Fig. 7 Using non-homogeneous structural models for modeling the variation of R_g with contrast: an example with casein micelles from fresh milk (FM_s1). The description of the core–shell models is in the text. (A) gives the variation of the apparent radius of gyration R_g (*i.e.*, including the contribution of fat droplets) as a function of D_2O content. In (B), we use a representation similar to the one used by Stuhrmann,[10] and that consists of plotting the squared radius of gyration of the casein micelle population $R_{g,CM}^2$ (*i.e.*, without the contribution of fat droplets) as a function of the reciprocal of the contrast of the micelles, $1/\overline{\rho_{CM}}$. Details about the calculation of $R_{g,CM}^2$ and $1/\overline{\rho_{CM}}$ from the experimental data are given in ESI part F.†

models clearly do not do better than the homogeneous model. Moreover, these models still show the small but systematic differences between the experimental and modeled data at low D_2O content (differences for which we do not have any satisfactory explanation yet). At first sight, these three models also give similar variations of the apparent radius of gyration R_g and a fair match to the experimental data. However, if we examine more closely the experimental series where the quantities of fat droplets are small, and consequently in which the variation of R_g is less impacted by these impurities, we can notice some small differences between the models (Fig. S8–S9 in the ESI†). This is illustrated in Fig. 7(A) for the experimental series FM_s1 where we observe a slight improvement of the fit with core–shell model 1. Conversely, the agreement is clearly less good with core–shell model 2 than with the other two models, essentially at high D_2O contents.

In Fig. 7(B), the results are plotted in a way that further confirms this small preference for a core–shell structural model in which the shell is less dense than the core. This type of representation is directly inspired from the 1974 classic work of H. B. Stuhrmann, where the author demonstrates that the variation of the squared radius of gyration of a core–shell object is a linear function of the reciprocal of its contrast. The slope of the linear fit to the data measures the internal heterogeneity of the structure, while the direction of the variation indicates whether the core is denser than the shell, or the opposite. In our case, building such a plot requires a separation of the contribution of the fat droplets from the total intensity, which can only be done accurately when this contribution is low compared to one of the casein micelles. Fig. 7(B) shows the plot for the sample set that has the lowest concentration of residual fat droplets. In this case, the contribution of the droplets is always less than ~8% of the total intensity, excepted in a very small range of contrasts that are in the immediate vicinity of the match point of casein micelles (*i.e.*, $0.40 < x_{D_2O} < 0.47$). Data in this range are not considered for the Stuhrmann plot since the contrast of the casein micelle is then too low for making the subtraction in an acceptable manner. From Fig. 7(B), it clearly appears that the squared radius of the casein micelle population, $R_{g,CM}^2$, has an overall trend to decrease as $1/\overline{\rho_{CM}}$ increases. Following Stuhrmann's theory, this indicates that, if the object is described as a core–shell particle, then the shell is less dense than the core. For comparison, we give in the same figure the variation of $R_{g,CM}^2$ for the three models that we introduced previously. Quite naturally, the model that is closest to the data is the one with a shell that is depleted in CaP nanoclusters (core–shell 1).

In ESI part F,† we provide Stuhrmann's plots equivalent to Fig. 7(B), but for the three other sets of experimental samples (Fig. S9–S11,† subfigures (A4), (B4) and (C4)). For the second set of samples prepared from fresh milk (FM_s2), the estimated quantity of fat droplets is significantly larger than that for the FM_s1 samples (Table S3†). However, there still exists a range of contrasts in which the contribution of the fat droplets is lower than 8–10% of the total intensity (Fig. S9†). In this range, the experimental points show the same trend as the one depicted in Fig. 7(B), further confirming the preference for the core–shell 1 model. As for the samples prepared from a powder (NPC_s1 and NPC_s2, Fig. S10–S11†), the quantity of fat is such that the contribution of the droplets to the total intensity is much larger than 8–10% for the vast majority of the experimental points (with percentages mainly comprised between 30–80%). In this case, the subtraction is not accurate enough to yield usable values of $R_{g,CM}^2$, and it is certainly too risky to interpret the variations of $R_{g,CM}^2$ with $1/\overline{\rho_{CM}}$.

Conclusion

The milk casein micelle is an intriguing object and the scientific community has always been in search of new ways for characterizing its structure. In this respect, the Stuhrmann analysis that we present in this paper is clearly among the approaches that still needed to be explored. A Stuhrmann analysis consists of examining how the SANS scattering intensity I_0 and the measured radius of gyration R_g of given objects vary with their contrast relative to the solvent (*i.e.*, the concentration of D_2O

over H_2O in the dispersion). These variations inform on the potential distribution of Scattering-Length Density SLD, and therefore composition, both between and within the particles. In the case of the casein micelle, information of this type is crucial for discriminating between structural models that assume different distributions of CaP nanoclusters within the micellar edifice.

The experimental work provided in this paper is the result of two extensive SANS campaigns, performed at an appropriate number of contrast points and with casein micelles of different origins. The obtained results show variations of R_g and I_0 that depend on the origin of the casein micelles and that are the sign of some distribution in composition between and/or within the objects present in the dispersions. From a rigorous and thorough examination of these variations, and coming back to the questions raised in the Introduction section, it appears that:

(1) The variation of R_g and I_0 with contrast is almost entirely explained through the coexistence of casein micelles and a minuscule quantity of objects (1 over 10^4 to 10^6 micelles) that are likely to be made of lipids or phospholipids (residual fat droplets and/or phospholipid vesicles). In particular, the presence of such non-casein particles in our dispersions is the only possible explanation for the minimum values of intensity recorded at the lowest contrasts, these values being clearly not compatible with the small natural variation of composition between casein micelles.

(2) The presence of remaining fat droplets readily explains why the apparent radius of gyration increases in the vicinity of the contrast match point of the micelle. In this region, the contribution of the fat droplets to the scattered intensity becomes significant. The measured R_g then gets closer to the average R_g of the population of fat droplets, which are overall slightly larger than the micelles. We demonstrate that the variation of R_g produced by the fat droplets is in all cases much stronger than the R_g variation that could possibly result from radial SLD heterogeneities within the micelle.

(3) For dispersions prepared from fresh milk, the contribution from fat droplets is reduced to the point where it can be subtracted from the total scattered intensity. In that case, a Stuhrmann analysis of the variation of the subtracted intensity with contrast can be performed. The results of this analysis are in favor of a core–shell casein micelle with a uniform radial distribution of CaP within its core and with an external κ-casein shell of ~10 nm that does not contain any CaP nanoclusters. This picture is fully consistent with the view of a micellar core that is made of a homogeneous network of caseins in which the CaP nanoclusters are randomly distributed.[3,13,24] It is also in accordance with some more recent models of a "sponge-like" casein micelle in which water-filled cavities are also present within the micellar core, thus similarly leading to a uniform radially averaged distribution of composition within the core.[1,2,7,8]

Acknowledgements

We thank F. Gaucheron, C. Lopez, and F. Guyomarc'h for helpful discussions, J. Li and T. Narayanan for the SAXS experiments at ESRF, and F. Rousseau and M. Haertlein for assistance in the preparation of the samples. We are also grateful to B. Robert for having collected the milk for this study. The Institut Laue-Langevin is acknowledged for financial support and provision of SANS beam time.

References

1 D. G. Dalgleish, *Soft Matter*, 2011, **7**, 2265–2272.
2 A. Bouchoux, G. Gésan-Guiziou, J. Pérez and B. Cabane, *Biophys. J.*, 2010, **99**, 3754–3762.
3 C. G. de Kruif, T. Huppertz, V. S. Urban and A. V. Petukhov, *Adv. Colloid Interface Sci.*, 2012, **171–172**, 36–52.
4 C. Holt, *Adv. Protein Chem.*, 1992, **43**, 63–151.
5 D. S. Horne, *Curr. Opin. Colloid Interface Sci.*, 2006, **11**, 148–153.
6 A. Shukla, T. Narayanan and D. Zanchi, *Soft Matter*, 2009, **5**, 2884–2888.
7 D. J. McMahon and B. S. Oommen, *J. Dairy Sci.*, 2008, **91**, 1709–1721.
8 R. Trejo, T. Dokland, J. Jurat-Fuentes and F. Harte, *J. Dairy Sci.*, 2011, **94**, 5770–5775.
9 R. Mezzenga and P. Fischer, *Rep. Prog. Phys.*, 2013, **76**, 046601.
10 H. Stuhrmann, *J. Appl. Crystallogr.*, 1974, **7**, 173–178.
11 C. G. De Kruif, *J. Dairy Sci.*, 1998, **81**, 3019–3028.
12 M. Ouanezar, F. Guyomarc'h and A. Bouchoux, *Langmuir*, 2012, **28**, 4915–4919.
13 C. Holt, C. G. De Kruif, R. Tuinier and P. A. Timmins, *Colloids Surf., A*, 2003, **213**, 275–284.
14 C. Holt, P. A. Timmins, N. Errington and J. Leaver, *Eur. J. Biochem.*, 1998, **252**, 73–78.
15 P. Walstra, *J. Dairy Res.*, 1979, **46**, 317–323.
16 J. Farrell, E. L. Malin, E. M. Brown and P. X. Qi, *Curr. Opin. Colloid Interface Sci.*, 2006, **11**, 135–147.
17 A. Le Parc, J. Léonil and E. Chanat, *BMC Cell Biol.*, 2010, **11**, 65.
18 R. Colsenet, O. Soderman and F. Mariette, *Macromolecules*, 2005, **38**, 9171–9179.
19 A. Bouchoux, P. Qu, P. Bacchin and G. Gésan-Guiziou, *Langmuir*, 2014, **30**, 22–34.
20 D. G. Dalgleish and M. Corredig, *Annu. Rev. Food Sci. Technol.*, 2012, **3**, 449–467.
21 P. Qu, G. Gésan-Guiziou and A. Bouchoux, *J. Membr. Sci.*, 2012, **417–418**, 10–19.
22 A. Sahu, N. Kasoju and U. Bora, *Biomacromolecules*, 2008, **9**, 2905–2912.
23 P. C. Shekar, S. Goel, S. D. S. Rani, D. P. Sarathi, J. L. Alex, S. Singh and S. Kumar, *Proc. Natl. Acad. Sci.*, 2006, **103**, 8000–8005.
24 S. Marchin, J. L. Putaux, F. Pignon and J. Léonil, *J. Chem. Phys.*, 2007, **126**, 045101–045110.
25 C. Moitzi, A. Menzel, P. Schurtenberger and A. Stradner, *Langmuir*, 2011, **27**, 2195–2203.
26 F. Pignon, G. Belina, T. Narayanan, X. Paubel, A. Magnin and G. Gésan-Guiziou, *J. Chem. Phys.*, 2004, **121**, 8138–8146.

27 W. Heller, *Acta Crystallogr., Sect. D: Biol. Crystallogr.*, 2010, **66**, 1213–1217.
28 S. Hansen, R. Bauer, S. B. Lomholt, K. B. Quist, J. S. Pedersen and K. Mortensen, *Eur. Biophys. J.*, 1996, **24**, 143–147.
29 A. J. Jackson and D. J. McGillivray, *Chem. Commun.*, 2011, **47**, 487–489.
30 P. H. Stothart and D. J. Cebula, *J. Mol. Biol.*, 1982, **160**, 391–395.
31 P. H. Stothart, *J. Mol. Biol.*, 1989, **208**, 635–638.
32 R. Gebhardt, T. Steinhauer, P. Meyer, J. Sterr, J. Perlich and U. Kulozik, *Faraday Discuss.*, 2012, **158**, 77–88.
33 T. Huppertz, M. A. Smiddy and C. G. De Kruif, *Biomacromolecules*, 2007, **8**, 1300–1305.
34 A. Pierre, J. Fauquant, Y. Le Graët, M. Piot and J. L. Maubois, *Lait*, 1992, **72**, 461–474.
35 P. Schuck, M. Piot, S. Méjean, Y. Le Graët, J. Fauquant, G. Brulé and J. L. Maubois, *Lait*, 1994, **74**, 375–388.
36 A. Bouchoux, P. E. Cayemitte, J. Jardin, G. Gésan-Guiziou and B. Cabane, *Biophys. J.*, 2009, **96**, 693–706.
37 R. Jenness and J. Koops, *Neth. Milk Dairy J.*, 1962, **16**, 153–164.
38 C. Holt, *J. Dairy Sci.*, 1998, **81**, 2994–3003.
39 J. Kohlbrecher and I. Bressler, *SASfit*, https://kur.web.psi.ch/sans/SANSSoft/sasfit.html, 2013.
40 P. V. Konarev, V. V. Volkov, A. V. Sokolova, M. H. J. Koch and D. I. Svergun, *J. Appl. Crystallogr.*, 2003, **36**, 1277–1282.
41 M. Malmstem, B. Bergenstähl, L. Nyberg and G. Odham, *J. Am. Oil Chem. Soc.*, 1994, **71**, 1021–1026.
42 W. Knoll, K. Ibell and E. Sackmann, *Biochemistry*, 1981, **20**, 6379–6383.
43 R. Waninge, E. Kalda, M. Paulsson, T. Nylander and B. Bergenståhl, *Phys. Chem. Chem. Phys.*, 2004, **6**, 1518–1523.
44 C. Gaiani, P. Schuck, J. Scher, J. J. Ehrhardt, E. Arab-Tehrany, M. Jacquot and S. Banon, *J. Food Eng.*, 2009, **94**, 130–134.
45 R. Tuinier and C. G. De Kruif, *J. Chem. Phys.*, 2002, **117**, 1290–1295.